

Generation of spin currents via Raman scattering

Ali Najmaie,^{1,*} E. Ya. Sherman,¹ and J. E. Sipe¹

¹*Department of Physics and Institute for Optical Sciences,
University of Toronto, 60 St. George St., Toronto, Ontario, Canada M5S 1A7*

(Dated: November 8, 2018)

We show theoretically that stimulated spin flip Raman scattering can be used to inject spin currents in doped semiconductors with spin split bands. A pure spin current, where oppositely oriented spins move in opposite directions, can be injected in zincblende crystals and structures. The calculated spin current should be detectable by pump-probe optical spectroscopy and anomalous Hall effect measurement.

PACS numbers: 78.30.-j, 72.25.-b, 71.70.Ej

Spintronics is the strategy of using the spins of carriers in solid state structures as a new degree of freedom to carry and transform information [1]. An important capability is the generation of spin currents, which couple spin and charge. Suggestions for the generation of spin currents have included proposals based on the use of the extrinsic and intrinsic spin Hall effects, as well as spin pumping [2, 3, 4]. All-optical generation and control of spin currents have also been proposed and observed [5, 6, 7, 8, 9]. In these optical schemes, the generation of the spin current is accompanied by the deposition of photon energies of about 1 eV per carrier in the system. Most of this energy is used simply to generate the electron-hole pairs, and is lost in the sense that it does not contribute to the motion of the carriers. An obvious goal for the all-optical manipulation of spin is the minimization of such energy loss.

Here we propose a new scheme for generating spin currents in doped semiconductors via a two photon Raman scattering process [10, 11], which can be understood as the absorption of a photon of frequency ω_1 and the emission of a photon at ω_2 . This process deposits an energy of $\hbar\Omega = \hbar(\omega_1 - \omega_2)$ per carrier in the crystal, which for GaAs is only about 0.5 meV. In the presence of spin splitting of the bands, stimulated spin-flip Raman scattering can produce a pure spin current, where electrons with opposite spins move in opposite directions. Hence no net charge current is injected.

Crucial to this effect is the spin-splitting of states, which results from the lack of inversion symmetry of the crystal. A schematic picture of the conduction states is shown in Fig. 1, where E_F denotes the Fermi energy. For simplicity we take the temperature to be zero [12]. The proposal in this letter is based on optically inducing transitions between states $d(\pm\mathbf{k})$ and $u(\pm\mathbf{k})$ at $\pm\mathbf{k}$ wavevectors, as depicted in Fig. 1, via Raman scattering. As an example, we first consider an optical field $\mathbf{E} = \mathbf{E}(\omega_1)e^{-i\omega_1 t} + \mathbf{E}(\omega_2)e^{-i\omega_2 t} + c.c.$ in the material, where $c.c.$ denotes complex conjugation and $\omega_1 > \omega_2$ and then present an experimentally relevant scenario of pulse excitation. The interaction of this field with the crystal in the dipole approximation is described by

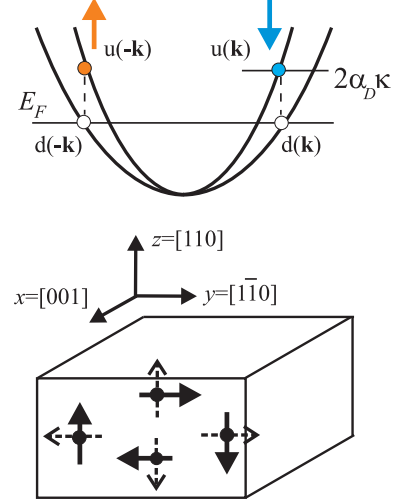


FIG. 1: (Color online) Schematic picture of the spin-split conduction bands. Spin-flip Raman scatterings correspond to transitions from $d(\pm\mathbf{k})$ to $u(\pm\mathbf{k})$ at $\pm\mathbf{k}$. The carriers at $u(\pm\mathbf{k})$ then have opposite spin orientations and hence a pure spin current is injected in the system. An example of the generated spin current is presented where two pure spin currents with orthogonal velocities are shown schematically. The dotted lines correspond to the velocities of the carriers, and the thick arrows depict their spins.

$H_{int} = -(e/mc)\mathbf{p} \cdot \mathbf{A}(t)$, where $e(m)$ is the charge(mass) of an electron, c is the speed of light and $\mathbf{A}(t)$ is the vector potential associated with the field. In the ground state $|0\rangle$, electrons occupy states up to the Fermi level. The wavefunction of the perturbed system at time t is then written as $|\Psi(t)\rangle = c_0(t)|0\rangle + \sum_{\mathbf{k}} c_{\mathbf{k}}(t)|eh\mathbf{k}\rangle$, where $|eh\mathbf{k}\rangle$, denotes the state where an electron (e) and hole (h) are generated at point \mathbf{k} (see Fig. 1). Time dependent perturbation theory is used to evaluate $c_{\mathbf{k}}(t)$ and hence to describe the rate of change in the expectation value of a single particle operator θ in the independent particle approximation,

$$\frac{\partial\langle\theta\rangle}{\partial t} = \sum_{\mathbf{k}} \langle eh\mathbf{k}|\theta|eh\mathbf{k}\rangle \frac{\partial(c_{\mathbf{k}}(t)c_{\mathbf{k}}^*(t))}{\partial t}. \quad (1)$$

This leads to the evaluation of injection rates of interest, including that for the density of flipped spins and for the spin current density [13]. The former can be written as

$$\frac{\partial n}{\partial t} = \xi^{abcd}(\omega_1, \Omega) E^a(\omega_1) E^{b*}(\omega_2) E^{c*}(\omega_1) E^d(\omega_2), \quad (2)$$

where $\xi^{abcd}(\omega_1, \Omega) = V^{-1} \sum_{\mathbf{k}} \Gamma^{abcd}(\mathbf{k}) \delta(\Omega - \omega_{eh}(\mathbf{k}))$ and

$$\Gamma^{abcd}(\mathbf{k}) = \left(\frac{\sqrt{2\pi} e^2}{\hbar^2 \omega_2 \omega_1} \right)^2 \left\{ \left[\sum_n \frac{v_{nh}^a(\mathbf{k}) v_{en}^b(\mathbf{k})}{\omega_1 + \omega_{hn}(\mathbf{k})} - \sum_n \frac{v_{en}^a(\mathbf{k}) v_{nh}^b(\mathbf{k})}{\omega_1 - \omega_{en}(\mathbf{k})} \right] \times (a \rightarrow c, b \rightarrow d)^* \right\}. \quad (3)$$

Here $\omega_{nm} = \omega_n - \omega_m$, V is the normalization volume, a, b, c and d are the Cartesian indices and $\mathbf{v}_{nm}(\mathbf{k})$ is the velocity matrix element between single particle states n and m at \mathbf{k} . Repeated indices are summed over. To quantify the spin current density J_{ab} , we use the conventional [14, 15] single particle spin current operator $j_{ab} = (1/2)(v^a S^b + S^b v^a)$, where $\mathbf{S} = \hbar \boldsymbol{\sigma}/2$ and $\boldsymbol{\sigma} = (\sigma^x, \sigma^y, \sigma^z)$ are the Pauli matrices. The spin current density injection rate is

$$\frac{\partial J_{ab}}{\partial t} = \mu^{abcdfg}(\omega_1, \Omega) E^c(\omega_1) E^{d*}(\omega_2) E^{f*}(\omega_1) E^g(\omega_2), \quad (4)$$

where $\mu^{abcdfg}(\omega_1, \Omega) = V^{-1} \sum_{e, h, \mathbf{k}} \delta j_{ab} \Gamma^{cdfg}(\mathbf{k}) \delta(\Omega - \omega_{eh}(\mathbf{k}))$ and $\delta j_{ab} = \langle e\mathbf{k} | j_{ab} | e\mathbf{k} \rangle - \langle h\mathbf{k} | j_{ab} | h\mathbf{k} \rangle$ is the spin current contribution per spin flip [16]. Both the fourth rank tensor $\xi^{abcd} = \xi^{cdab}$ and sixth rank pseudotensor $\mu^{abcdfg} = \mu^{abfgcd}$ can be shown to be real by using time reversal symmetry; the T_d symmetry group of the crystal can be used to deduce the non-zero and independent tensor components. To calculate the tensors, we describe the spin splitting of the conduction states by the Dresselhaus Hamiltonian in the Γ point basis $\{|1/2, 1/2\rangle, |1/2, -1/2\rangle\}$

$$H = \frac{\hbar^2 k^2}{2m_c} + \alpha_D \boldsymbol{\kappa} \cdot \boldsymbol{\sigma}, \quad (5)$$

where $\kappa_x = k_x(k_y^2 - k_z^2)$ and $\kappa_{y,z}$ are cyclic permutation of κ_x , $\alpha_D = 27.6 \text{ eV}\text{\AA}^3$ is the Dresselhaus parameter and $m_c = 0.067m$ is the electron effective mass [17, 18]. The spin splitting at wavevector \mathbf{k} is $2\alpha_D \boldsymbol{\kappa}$. The valence states of the semiconductor serve as the intermediate virtual states n in Eq. (3). The heavy and light valence states are modelled using the isotropic 4×4 Luttinger-Kohn Hamiltonian, with the Luttinger parameters $\gamma_1 = 6.85$ and $\gamma = (\gamma_2 + \gamma_3)/2 = 2.5$. The split-off band is described by a diagonal 2×2 Hamiltonian, with the effective mass taken to be $0.154m$ [19]. A band gap energy of $E_g = 1.51 \text{ eV}$ and a split-off energy of 0.34 eV are used. The Fermi energy of the electrons in

the conduction band is given by $E_F = E_g + \hbar^2 k_F^2 / 2m_c$, where $k_F = (3\pi^2 N)^{1/3}$ for the carrier concentration N ; we use a concentration of $N = 10^{18} \text{ cm}^{-3}$ in the calculations. The speed of the injected carriers is given by $v_F = \hbar k_F / m_c \approx 500 \text{ km/s}$. The intraband velocity matrix elements are evaluated using $\mathbf{v} = \hbar^{-1} \partial H(\mathbf{k}) / \partial \mathbf{k}$ as the velocity operator. We use a Kane parameter $P = (\hbar/m) \langle S | p_x | X \rangle = 10.49 \text{ eV}\text{\AA}$ [19] and numerically evaluate the tensor components.

Spin orbit coupling splits the Fermi-surface into two surfaces. The fraction of the electrons that are contained in the region between the two surfaces is given by $\approx 2m_c \alpha k_F / \hbar^2$ and is about 1% of the free carriers available in the system at $N = 10^{18} \text{ cm}^{-3}$. Only this fraction of the free carriers in the system is subject to Raman scattering. This sets a limit of $\approx 10^{-2} N$ on the concentration of carriers that can contribute to the injected current.

Spin flip Raman scattering has typically been studied using orthogonally polarized fields $\mathbf{E}(\omega_{1,2})$ [11]. Hereafter we use the following definition of the coordinates, $\hat{x} \equiv [001]$, $\hat{y} \equiv [1\bar{1}0]$ and $\hat{z} \equiv [110]$ and consider more general fields normally incident on a crystal with a $[110]$ growth axis

$$\mathbf{E}(\omega_{1,2}) = E_{1,2} \beta_{1,2} (\cos(\rho_{1,2}^x) \hat{x} + i \cos(\rho_{1,2}^y) \hat{y}), \quad (6)$$

for phases $(\rho_1^x, \rho_1^y, \rho_2^x, \rho_2^y)$, and normalization factors $\beta_{1,2}$. This allows the most general analysis of the fields polarizations. We find the spin-flip and spin current density injection rates

$$\begin{aligned} \frac{\partial n}{\partial t} &= g \cdot A_{\varepsilon_1}(\Omega) I_1 I_2, \\ \frac{\partial J_{yz}}{\partial t} &= g \cdot \frac{\hbar}{2} [B_{\varepsilon_1}(\Omega) + C_{\varepsilon_1}(\Omega)] I_1 I_2, \\ \frac{\partial J_{zy}}{\partial t} &= g \cdot \frac{\hbar}{2} [B_{\varepsilon_1}(\Omega) - C_{\varepsilon_1}(\Omega)] I_1 I_2, \end{aligned} \quad (7)$$

where $g = (\beta_1 \beta_2)^2 (\cos(\rho_1^y) \cos(\rho_2^x) + \cos(\rho_1^x) \cos(\rho_2^y))^2$, and $I_{1,2}$ are the incident intensity of the $\varepsilon_{1,2} = \hbar \omega_{1,2}$ components of the fields. Here A_{ε_1} , B_{ε_1} and C_{ε_1} are linear combination of the tensor components ξ^{abcd} and μ^{abcdfg} . The mismatch in the dielectric function ϵ across the interface leads to a ratio $2/(\sqrt{\epsilon} + 1)$ of the electric fields in the crystal and air. Two pure spin currents are injected in the crystal, one injected along $y = [1\bar{1}0]$ with spins parallel to $z = [110]$ and another injected along $z = [110]$ with spins pointing parallel to $y = [1\bar{1}0]$ (Fig. 1). Clearly for either right (or left) circularly (e.g. $\beta_1 = \beta_2 = 1/\sqrt{2}$, $\rho_1^x = \rho_2^x = 0$, $\rho_1^y = \rho_2^y = 0$ (or π)) and cross-linearly (e.g. $\beta_1 = \beta_2 = 1$, $\rho_1^x = \rho_2^x = 0$, $\rho_1^y = \rho_2^y = \pi/2$) polarized fields, the same spin currents are injected. Moreover, for co-linearly polarized fields, where $g = 0$, no spin-flips and hence no pure spin current can be induced.

First we consider the case where the photon energy $E_1 = \hbar \omega_1 = 0.754 \text{ eV}$ is close $E_g/2$. All two photon

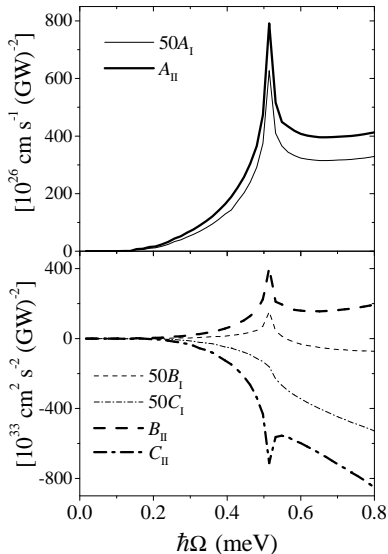


FIG. 2: The thin lines show the coefficients, A_I , B_I and C_I Eq. (7) for $\Omega = \omega_1 - \omega_2$ and $\hbar\omega_1 = 0.754$ eV, about half the band gap. The thick lines show the coefficients, A_{II} , B_{II} and C_{II} Eq. (7) for $\hbar\omega_1 = 1.49$ eV, about 20 meV below the band gap.

absorption from the valence to the conduction bands is avoided in this scenario. In Fig. 2, we present A_I , B_I and C_I . The role of the resonance enhancement can be investigated by using optical fields of energy $E_{II} = \hbar\omega_1 = 1.49$ eV close to the band gap. Transitions from the partially filled conduction band to the higher bands are avoided at this energy, but two photon excitations from the valence states to conduction states are allowed. Nonetheless these transitions are away from the Γ point and should not contribute to the injected pure spin current from the spin flip Raman processes we discuss in this letter. The two photon absorption is estimated to be an order of magnitude smaller than the spin-flip injection rate discussed here [20], and excitons are not generated. The carrier and spin current density injection rates characterized by A_{II} , B_{II} and C_{II} are presented in Fig. 2. The sharp features in the results, shown in Fig. 2, correspond to the van Hove singularities in the joint density of states for the spin-flip transitions. The van Hove singularity is due to the vanishing derivative in the spin splitting, $2\alpha_D \nabla_{\mathbf{k}} \kappa$ along high symmetry directions, and an analysis of the Dresselhaus Hamiltonian shows that the resulting density of states increases as $\ln(1/|\Omega - \Omega_{vH}|)$, where Ω_{vH} is the position of the singularity. To this point we have discussed the injection rate of pure spin currents by stimulated Raman scattering using two nominally continuous wave (CW) beams at distinct frequencies ω_2 and $\omega_1 > \omega_2$. We now turn to the ultrafast pulse regime, and stress that a pure spin current can be injected through the Raman effect

by a single pulse, with the scattering now arising from the spectral width of the pulse. For a pulse with a centre frequency ω_0 and width $\Delta\omega$, if we have $\omega_0 \gg \Delta\omega$ and $\omega_0 \gg \Omega_{\max}$, where $\hbar\Omega_{\max}$ is the maximum spin splitting, the straightforward generalization of the calculation in Eqs. (2) and (4) leads to the injection of densities of spin flips and spin current given by

$$\Delta n = \int_0^{\Omega_{\max}} \frac{d\Omega}{2\pi} \xi^{abcd}(\omega_0, \Omega) G^{abcd}(\Omega), \quad (8)$$

$$\Delta J_{ab} = \int_0^{\Omega_{\max}} \frac{d\Omega}{2\pi} \mu^{abcdfg}(\omega_0, \Omega) G^{cdfg}(\Omega), \quad (9)$$

where the field correlation function for $\mathbf{E}(t) = (2\pi)^{-1} \int_{-\infty}^{\infty} d\omega \mathbf{E}(\omega) e^{-i\omega t}$ is

$$G^{abcd}(\Omega) = \int_0^{\infty} \frac{d\omega_1 d\omega'_1}{(2\pi)^2} E^a(\omega_1) E^{b*}(\omega_1 - \Omega) E^{c*}(\omega'_1) E^d(\omega'_1 - \Omega). \quad (10)$$

We consider a (right or left) circularly polarized short pulse of the form $E(t) = 2E_0 \exp(-t^2/\tau^2) \cos(\omega_0 t)$, with fluence (pulse energy per unit area) F . A short pulse [21] ($\tau\Omega_{\max} \ll 1$ and $\tau \ll \mu m_c/|e|$, where μ is the mobility) essentially leads to the generation of the spin current in the ballistic limit. For $\hbar\omega_0 = 0.754$ eV (corresponding to A_I , B_I and C_I in Fig. 2), the density of spin flips per pulse is $\Delta n_I \approx (1.8 \times 10^{20} \text{cm}^3/J^2) F^2$, which gives $\Delta n_I \approx 10^{15} \text{cm}^{-3}$ for an experimentally accessible fluence of $F = 3 \times 10^{-3} J/\text{cm}^2$. In a scenario where $\hbar\omega_0 = 1.49$ eV (corresponding to A_{II} , B_{II} and C_{II} in Fig. 2) the spin flips density due to Raman scattering is $\Delta n_{II} \approx (1.2 \times 10^{22} \text{cm}^3/J^2) F^2$; a spin flip density of $\Delta n_{II} \approx 10^{15} \text{cm}^{-3}$ can be achieved for a fluence of $F = 3 \times 10^{-4} J/\text{cm}^2$, which reflects a resonance enhancement of the process by two orders of magnitude.

Note that the injection in this process is proportional to F^2 , whereas from Eq. (7) for nominal CW irradiation one might expect a scaling with $I_{\max}^2 \tau \propto F^2/\tau$ where I_{\max} is the maximum intensity in the pulse. The reason is that, for $\Omega_{\max} \tau \ll 1$, a factor $\Omega_{\max} \tau \approx \Omega_{\max}/\Delta\omega$ appears in the final result following from Eqs. (8) and (9), reflecting the fact that only a fraction $\Omega_{\max}/\Delta\omega$ of the pulse bandwidth can contribute to the Raman scattering.

With each pulse a number of carriers $\approx \Delta n \times S\eta$ are excited, where S is the laser spot area and η is the penetration depth. In earlier experiments [5, 6] involving interband transitions, a large number of carriers are available in the valence states, and typically $\approx (10^{18} \text{cm}^{-3}) S\eta$, where $\eta \approx 1 \mu\text{m}$, carriers can contribute to the spin currents. On the other hand, in Raman injected spin currents the penetration depth is much larger than that for

interband transitions, with a limit $\eta' \approx 10^3 \mu\text{m}$ set by the Drude absorption due to free carriers. This allows a large $\approx (10^{15} \text{cm}^{-3})S\eta'$ number of spin flips in the sample, which will then contribute to the injected pure spin current.

Pump and probe schemes have been used to experimentally observe injected pure spin currents [6]. An experimentally relevant parameter in these schemes is the separation between the opposite spins after momentum relaxation. This distance can be estimated by $d^a = (2\mu m_c / |e\hbar|) \sum_b |J_{ab}| / \dot{n}$ [22, 23]. For circularly polarized as well as cross linearly polarized fields, a spin separation of $d^y \approx 18 \text{ nm}$ for $\mu \approx 5 \times 10^3 \text{ cm}^2/(\text{Vs})$ is predicted, a distance which is within experimental capabilities [6]. Measuring a pure spin current by using the anomalous spin Hall effect arising due to skew scattering by impurities [24, 25] has also been proposed [8]. The spin current J_{ab} causes a spin-Hall bias V_{sH} along the direction perpendicular to the electron propagation. This bias is estimated as $V_{sH} \approx \tan(\theta_{sH})V_{\text{eff}}$, where θ_{sH} is the spin-Hall angle and V_{eff} is the effective bias that would cause a current density eJ_{ab}/\hbar ; it is of the order of $e\Delta n v_F$, where Δn is the number of carriers that form the pure spin current. Therefore $V_{\text{eff}} \approx L(\Delta n/N)v_F/\mu$, where $L \approx 10 \mu\text{m}$ is the lateral size of the system, which is assumed to be approximately equal to the spot size. The ratio $\Delta n/N$ is estimated as $\zeta \alpha_D k_F^3/E_F$, where ζ is the fraction of Raman accessible electrons that undergo a spin flip. With the above mobility we obtain: $V_{\text{eff}}/L \approx 10\zeta \text{ V/cm}$. The above analysis shows ζ to be about 0.1. With the angle θ_{sH} estimated by Abakumov and Yassievich [24] for GaAs at low temperatures as $\theta_{sH} \approx 10^{-3}$, we obtain an upper estimate of $V_{sH} \approx 10^{-6} \text{ V}$.

In conclusion, stimulated spin-flip Raman scattering can be used to inject spin currents in doped semiconductors with spin splitting. We have considered the case of an n -doped GaAs bulk crystal, and showed that the injected spin current is a pure spin current comprised of spins with opposite orientations travelling in opposite directions. This pure spin current should be experimentally accessible, and can be achieved either with two continuous waves contributing to the Raman scattering, or by using a single pulse. The scheme is all-optical but, unlike other optical schemes involving the excitation of electron-hole pairs, here there is minimal energy deposited in the crystal. The system is thus only slightly perturbed from equilibrium, and the description of transport and the design of device structures should be easier than in scenarios employing other optical schemes. High mobility quantum wells should provide ideal testing grounds for the general proposal discussed in this letter.

A.N. acknowledges support from an OGS. This work was supported in part by the NSERC (Canada) and DARPA. We thank D. Luxat, P.A. Marsden, J. Hübner,

H.M. van Driel, and A.L. Smirl for useful discussions.

* Electronic address: anajmaie@physics.utoronto.ca

- [1] *Optical Orientation*, edited by F. Meier and B. P. Zakharchenya, Modern Problems in Condensed Matter Sciences, Vol. **8** (North-Holland, Amsterdam, 1984).
- [2] Y. K. Kato, *et al.*, Science, **306**, 1910 (2004).
- [3] J. Wunderlich, *et al.*, Phys. Rev. Lett. **94**, 047204 (2005).
- [4] S. K. Watson, *et al.*, Phys. Rev. Lett. **91**, 258301 (2003).
- [5] J. Hübner, *et al.*, Phys. Rev. Lett. **90**, 216601 (2003).
- [6] M. J. Stevens, *et al.*, Phys. Rev. Lett. **90**, 136603 (2003).
- [7] R.D.R. Bhat, *et al.*, Phys. Rev. Lett. **94**, 096603 (2005).
- [8] E. Ya. Sherman, A. Najmaie and J.E. Sipe, Appl. Phys. Lett. **86**, 122103 (2005)
- [9] S.D. Ganichev and W. Prettl, J. Phys. Cond. Matter **15**, R935 (2003).
- [10] B. Jusserand, *et al.*, Phys. Rev. Lett. **69**, 848 (1992).
- [11] D.C. Hamilton and A.L. McWhorter, in *Light Scattering Spectra of Solids*, Edited by G.B. Wright (Springer-Verlag, 1969) p. 297, M.V. Klein in *Light Scattering in Solids*, Edited by M. Cardona, Topics in Applied Physics. Vol. 8, Chp. 4 (Springer-Verlag, 1975).
- [12] While we only consider the Stokes Raman process, the thermal spreading of the Fermi distribution in both spin-split bands will allow for anti-Stokes processes. However, the combination of the Stokes and anti-Stokes contributions can be shown to be weakly temperature dependent.
- [13] H.M. van Driel and J.E. Sipe, in *Ultrafast Phenomena in Semiconductors*, Edited by K-T. Tsen (Springer, Berlin, 2001), Chp. 5.
- [14] E. I. Rashba, Phys. Rev. B **70**, 161201 (2004).
- [15] S. I. Erlingsson, J. Schliemann, and D. Loss, Phys. Rev. B **71**, 035319 (2005).
- [16] In this letter we neglect the uncertainty in the momentum dependent spin-splitting; which is allowed since the momentum is a well-defined quantum number: the product $k_F l \approx 10$, where k_F is the Fermi wavevector and l is the mean free path. We also assume that the inelastic broadening of the states arising due to inelastic scatterings is small compared to $\alpha_D \kappa$ due to low T even at $k_B T > \alpha_D \kappa$ [10]. The role of relaxation processes in the Raman injection of spin current is, however, an interesting problem and requires a separate investigation.
- [17] G. Dresselhaus, Phys. Rev. **100**, 580 (1955).
- [18] R. Winkler, *Spin-Orbit Coupling Effects in Two-dimensional Electron and Hole systems*, (Springer, 2003).
- [19] J. P. Loehr, *Physics of Strained Quantum Well Lasers* (Kluwer Academic Publishers, Dordrecht, 1998).
- [20] R. Atanasov, *et al.*, Phys. Rev. Lett. **76**, 1703 (1996).
- [21] J.-Y. Bigot, *et al.*, Phys. Rev. Lett. **67**, 636 (1991).
- [22] The experimentally observed mobility at the assumed density and at 300 K is $\approx 3000 \text{ cm}^2/(\text{Vs})$. We take the mobility $5000 \text{ cm}^2/(\text{Vs})$ for the low temperatures considered here.
- [23] D. L. Rode, *Semiconductors and Semimetals*, R. K. Willardson and A. C. Beer, eds., Academic Press, N.Y., vol. 10, 1975, p. 1, and references therein.
- [24] V.N. Abakumov and I.N. Yassievich, Sov. Phys. JETPh **34**, 1375 (1972). [Zh. Exp. Theor. Phys. **61**, 2571 (1972)]
- [25] P. Nozieres and C. Lewiner, Journal de Physique **10**, 901

(1973).